Discrete-Time Model of an Induction Motor

J. Böcker

Abstract

If a state-space observer of a continuous-time process is to be realized on a sampling microprocessor system, a discrete time model of the process is needed. Time-varying continuous-time parameters require the on-line computation of the discrete-time model. For this purpose numerical integration algorithms are used to get an approximate model instead of the exact model in discrete-time. For the model of an induction motor it is pointed out that the often-used first-order algorithm of Euler (RK1) is crucial. Even the choice of the continuous-time differential equation system, which has to be discretized, influences the quality of the discrete-time approximation in a decisive manner. On the one hand even stability problems appear while on the other hand, by choosing the equation system in a skilful manner, one obtains a simple and accurate discrete-time model, which can be used for microprocessor implementations.

1 Introduction

For state observers, as well as for parameter estimation in state-space, a state-space model of the considered process is required. Often this process is continuous in time while the observer or parameter estimator is usually built up as a digital sampled data system in discrete-time. Hence the required model must be a discrete-time one. The evaluation of such a discrete-time model, starting from a given continuous-time one, is a standard problem in the theory of discrete-time systems.

In the case of linear systems the transition matrix gives the general solution of this problem [6]. Except for special cases where a closed solution can be found, the evalutation of the transition matrix requires extensive numerical computations. If possible, these computations should be done off-line, but even for linear but time-varying systems this approach is often not applicable. Also, continuous-time parameters may not vary with time, but are known only at run-time, or perhaps an on-line calibration is desired. In all these cases the transition matrix must be evaluated on-line using a microprocessor system with relatively small computing power, which usually has only a poor library of numerical subroutines.

Therefore, instead of "exact" discretisation, approximation methods are used. In the case of nonlinear systems this is mostly the only chance to get a solution. From the various numerical integration algorithms available [9, 13], the explicit algorithm of Euler (RK1) is often found in technical realisations [1, 2, 8, 11, 12]. This is a 1st-order approximation from the family of Runge-Kutta algorithms. It approximates the integration by stepwise summations. This algorithm is very simple, but its numerical performance is crucial.

This paper intends to point out the difficulties and limitations of such a RK1 discretisation, but it shows also that the quality of the RK1 approximation depends in a decisive manner on the choice of the continuous-time model. (For every system several models can be found, which cannot be converted into one other by a linear time-invariant transformation.) As an example the model of an induction motor is used.

2 Continuous-Time Model of an Induction Motor

We start from a mathematical model of an induction motor with the widely-used complex vector notation to describe two-dimensional real-valued state variables [4]:

$$\dot{\psi}_S^S(t) = -R_S i_S^S(t) + u_S^S(t), \tag{1}$$

$$\dot{\psi}_r^r(t) = -R_r i_r^r(t). \tag{2}$$

Here

ψ_S, ψ_r denote the stator and rotor magnetic flux linkages,
i_S, i_r the stator and rotor currents,
u_S the (external) stator voltage and
R_S, R_r denote the stator and rotor resistances.

The upper index indicates the reference system of a complex vector (**Fig. 1**). For example, i_S^S denotes the complex vector of the stator current in the reference system of the stator and i_S^r is the same current, but with respect to the rotating rotor system.

If linear inductances are assumed, the magnetic fluxes can be expressed in terms of the currents through

$$\psi_S(t) = L_S i_S(t) + M i_r(t), \tag{3}$$

$$\psi_r(t) = M i_S(t) + L_r i_r(t) \tag{4}$$

where L_S and L_r denote the stator and rotor self-inductances and M the mutual inductance. Because of the rotational symmetry of an induction motor these

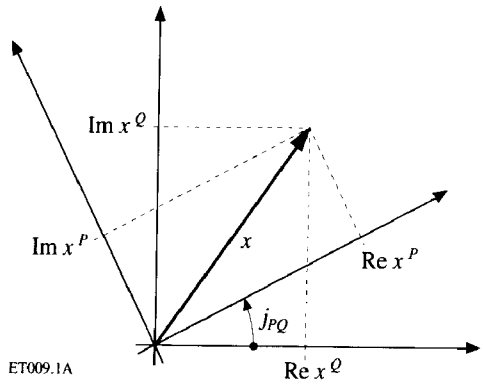

Fig. 1. Complex vector representation in various reference systems

equations are valid in every reference system so that the upper indices may be omitted here. Solving for the currents gives

$$i_s(t) = \frac{1}{\sigma L_s}\left(\psi_s - \frac{M}{L_r}\psi_r\right), \tag{5}$$

$$i_r(t) = \frac{1}{\sigma L_r}\left(\psi_r - \frac{M}{L_s}\psi_s\right) \tag{6}$$

where

$$\sigma := 1 - \frac{M^2}{L_s L_r} \tag{7}$$

is the leakage coefficient. Substituting the currents in eqs. (1) and (2), the differential equations (deqs.) become now

$$\dot{\psi}_s^s(t) = -\frac{R_s}{\sigma L_s}\psi_s^s(t) + \frac{R_s M}{\sigma L_s L_r}\psi_r^s(t) + u_s^s(t), \tag{8}$$

$$\dot{\psi}_r^r(t) = -\frac{R_r}{\sigma L_r}\psi_r^r(t) + \frac{R_r M}{\sigma L_s L_r}\psi_s^r(t). \tag{9}$$

In these equations the fluxes appear as state variables only, but with references to both stator and rotor systems.

For any complex vector $x(t)$, the relation between its representation in a reference system P and another reference system Q is given by

$$x^P(t) = e^{-j\varphi_{PQ}(t)}x^Q(t), \tag{10}$$

and for the time derivative $\dot{x}(t)$ by

$$\dot{x}^P(t) = -j\omega_{PQ}(t)x^P(t) + e^{-j\varphi_{PQ}(t)}\dot{x}^Q(t). \tag{11}$$

Here $\varphi_{PQ}(t) = -\varphi_{QP}(t)$ is the rotation angle of the system P measured from system Q in mathematical convention (Fig. 1) and

$$\omega_{PQ}(t) = \dot{\varphi}_{PQ}(t) \tag{12}$$

is the angular frequency.

With these relations, eq. (9) for the rotor voltage can be transformed into the stator reference system. Both deqs. are then obtained in a common reference system:

$$\dot{\psi}_s^s(t) = -\frac{R_s}{\sigma L_s}\psi_s^s(t) + \frac{R_s M}{\sigma L_s L_r}\psi_r^s(t) + u_s^s(t), \tag{13}$$

$$\dot{\psi}_r^s(t) = \left[-\frac{R_r}{\sigma L_r} + j\omega_{rs}(t)\right]\psi_r^s(t) + \frac{R_r M}{\sigma L_s L_r}\psi_s^s(t). \tag{14}$$

Now the angular frequency ω_{rs} (angular velocity of the rotor measured from the stator system) appears in eq. (14). If the angular frequency is constant, eqs. (13) and (14) become a system of linear time-invariant differential equations in canonical form:

$$\dot{\boldsymbol{x}}(t) = \boldsymbol{A}\boldsymbol{x}(t) + \boldsymbol{B}u(t). \tag{15}$$

From this the system and the input matrices can be identified as

$$\boldsymbol{A} = \begin{bmatrix} -\frac{R_s}{\sigma L_s} & \frac{R_s M}{\sigma L_s L_r} \\ \frac{R_r M}{\sigma L_s L_r} & -\frac{R_r}{\sigma L_r} + j\omega_{rs} \end{bmatrix}, \quad \boldsymbol{B} = \begin{bmatrix} 1 \\ 0 \end{bmatrix}, \tag{16}$$

using the state vector

$$\boldsymbol{x}(t) = \begin{bmatrix} x_1(t) \\ x_2(t) \end{bmatrix} = \begin{bmatrix} \psi_s^s(t) \\ \psi_r^s(t) \end{bmatrix} \tag{17}$$

and the input variable

$$u(t) = u_s^s(t). \tag{18}$$

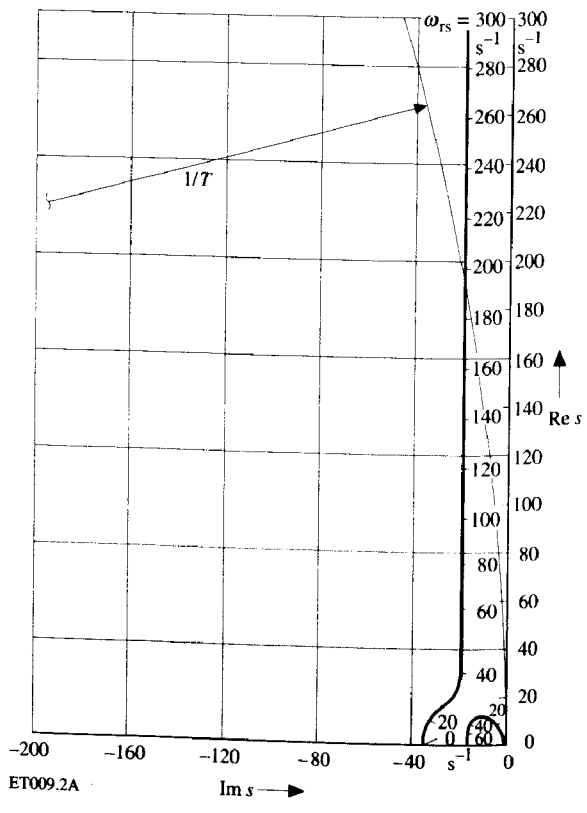

Fig. 2. Loci of eigenvalues of the continuous-time model of an induction motor with angular frequency as parameter

The state vector consists of complex-valued elements. This form is retained although it is possible to change from the 2nd-order complex-valued system to a 4th-order real-valued one. Because all mathematical tools such as Laplace transform or z-transform are also applicable to complex-valued functions in the time-domain [3] (although not usually used), there is no reason to do this. Of course, complex eigenvalues of such a system no longer appear as complex conjugate pairs.

Both eigenvalues of the above system were computed for a 1.2 MW induction motor example. The root loci are shown in **Fig. 2**. The parameter used is the angular frequency ω_{rs}. With increasing angular frequency the imaginary part of one eigenvalue tends to the angular frequency itself while the real part tends to the negative reciprocal value of the rotor leakage time constant

$$\tau_r := \sigma L_r / R_r , \tag{19}$$

which can be shown by limit calculations. Hence we find that for large angular frequencies this eigenvalue is approximated by

$$s_1 \approx -1/\tau_r + \mathrm{j}\,\omega_{rs} . \tag{20}$$

3 Discrete-Time Model of an Induction Motor by Means of RK1 Discretisation

Suppose the input function $u(t)$ is constant between sampling instants $t = kT$ (a zero-order hold). Then, with the transition matrix

$$\boldsymbol{\Phi} := \mathrm{e}^{AT} \tag{21}$$

and the discrete-time input matrix

$$\boldsymbol{H} := \int_0^T \mathrm{e}^{A\tau}\mathrm{d}\tau\, \boldsymbol{B}, \tag{22}$$

the discrete-time system of the deq.-system (15) is as follows:

$$\boldsymbol{x}((k+1)T) = \boldsymbol{\Phi}\,\boldsymbol{x}(kT) + \boldsymbol{H}u(kT). \tag{23}$$

As pointed out in the introduction, this model is not appropriate for on-line computations, because the transition matrix $\boldsymbol{\Phi}$ and the input matrix $\boldsymbol{H}$ have to be re-evaluated each time the angular frequency varies. The same problem occurs with variations in other parameters, for example, with a varying sampling period T.

Using instead the integration algorithm of Euler (RK1), the matrices $\boldsymbol{\Phi}$ and $\boldsymbol{H}$ are replaced by their 1st-order approximations

$$\hat{\boldsymbol{\Phi}} = \boldsymbol{I} + T\boldsymbol{A}, \tag{24}$$

$$\hat{\boldsymbol{H}} = T\boldsymbol{B} \tag{25}$$

where $\boldsymbol{I}$ denotes the identity matrix. However, the disadvantages of this algorithm are known: The stability domain of the RK1 algorithm in the (continuous-time) plane of eigenvalues is a circle with center at $-1/T$ and with radius $1/T$. This is obtained from the stability domain $|z| < 1$ of the plane of discrete-time eigenvalues via the inverse mapping of eq. (24) [5, 9] (see **Fig. 3**). All eigenvalues s_i of the continuous-time system must be located inside that circle to get a stable RK1 discretisation:

$$|s_i + 1/T| < 1/T. \tag{26}$$

If a continuous-time system has only stable eigenvalues (with negative real parts), but some of them are placed outside that circle, the RK1 discretisation is unstable. Crucial are those complex eigenvalues which are situated close to the imaginary axis. If the sampling period T is too large (the larger the sampling period the smaller the stability circle), these eigenvalues may come close to the stability boundary or may lie outside the stability circle. From eq. (26) an upper limit for the sampling period T can be derived as

$$T < T_{max} = \min_i \frac{-2\,\mathrm{Re}\,s_i}{|s_i|^2} \tag{27}$$

to guarantee stability of the discrete-time approximation of a given stable continuous-time system. An intuitively chosen sampling period, using for example $n = 10 \ldots 20$ samples per period of self-oscillation,

$$T = \min_i |2\pi / s_i| / n, \tag{28}$$

results in instability even with damping rates $-\mathrm{Re}\,s_i/|s_i|$ of 0.3 ... 0.15. This is the reason for the poor properties of the RK1 method in cases of weakly-damped oscillating systems. In Fig. 2 the stability circle is shown for $T = 1$ ms (its center lies outside the diagram) together with the loci of eigenvalues. Obviously the RK1 discretisation becomes unstable at an angular frequency of about 195 s^{-1}. To ensure stability, referring to

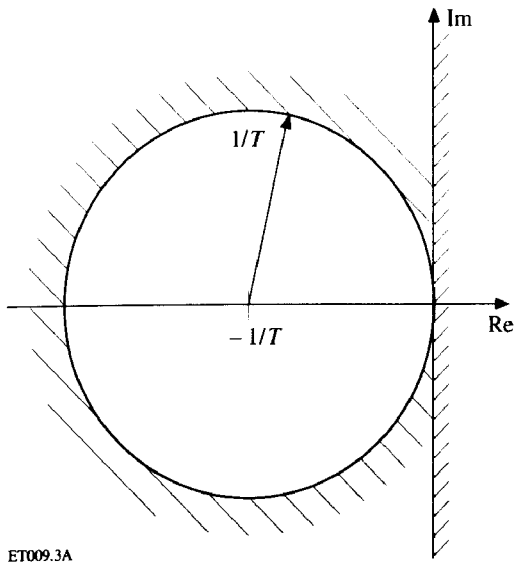

Fig. 3. Stability and instability domains of a RK1 discretisation in the plane of continuous-time eigenvalues

eqs.(27) and (20), the sampling period has to be smaller than

$$T_{max} \approx \frac{2 / \tau_r}{1 / \tau_r^2 + \omega_{rs}^2} \approx \frac{2}{\tau_r \omega_{rs}^2}. \quad (29)$$

Here the inverse proportionality of the maximum sampling period T_{max} and the leakage time constant τ_r is evident. Hence, especially for large motors with relatively large time constants, very small sampling periods are required to ensure stability. On the other hand, it is possible to get an appropriate result for small motors with small time constants using larger sampling periods. The considered motor has a leakage time constant of 53 ms. With a nominal angular frequency of $\omega_{rs} = 2\pi\, 50$ Hz this yields a maximum limit of

$$T_{max} \approx 0.38 \text{ ms}. \quad (30)$$

This corresponds to about 50 samples per period. This is a number for which one might assume instability would not be a problem at all. To ensure not only stability but also a good accuracy, an even smaller sampling period must be chosen.

To find a quantitative measure for assessing the precision, an error quantity consisting of the difference between a state variable $\hat{x}_i$ of the RK1 model and its value x_i in the "exact" discretisation is introduced. This is then related to the maximum value of the input sequence. Next a search for the maximum absolute value (better: supremum) over all sampling instants kT and all possible input sequences u is made:

$$\hat{\varepsilon}_i := \sup_u \frac{\sup_k |\hat{x}_i(kT) - x_i(kT)|}{\sup_k |u(kT)|}. \quad (31)$$

The supremum of the absolute values of a sequence is its L_∞ norm and it is denoted by $\|\cdot\|_\infty$. The operators of the mappings of the input sequence u onto the sequences of state variables x_i and $\hat{x}_i$ are defined:

$$\Gamma_i : u \to x_i, \quad \hat{\Gamma}_i : u \to \hat{x}_i. \quad (32)$$

Now the desired error quantity can be written as

$$\hat{\varepsilon}_i = \sup_u \frac{\|\hat{x}_i - x_i\|_\infty}{\|u\|_\infty} = \sup_u \frac{\|\hat{\Gamma}_i u - \Gamma_i u\|_\infty}{\|u\|_\infty} = \sup_u \frac{\|(\hat{\Gamma}_i - \Gamma_i)u\|_\infty}{\|u\|_\infty},$$

$$\hat{\varepsilon}_i = \|\hat{\Gamma}_i - \Gamma_i\|_\infty. \quad (33)$$

The last term is the L_∞ norm of an operator. It can be evaluated through the absolute sum of the corresponding weighting sequence (the pulse response sequence) [3].

In the example considered, the rotor flux $x_2 = \psi_r^s$, is of main interest, since knowing this state variable enables the realisation of various control strategies for induction motors. For this state variable the error quantity was computed as a function of the angular frequency and for various sampling periods (see **Fig. 4**). The instability, already known from the results of the eigenvalues, is seen here as an error increasing

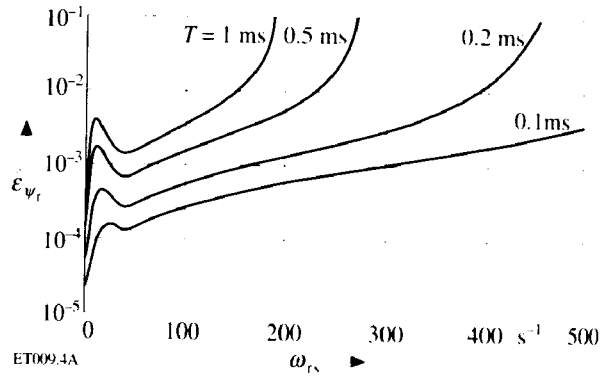

Fig. 4. Error quantity $\hat{\varepsilon}_{\psi_r}$ of model $(\hat{\Phi}, \hat{H})$ versus angular frequency ω_{rs}

over all limits. The local error maximum, at about $\omega_{rs} \approx 10\ s^{-1}$, is caused by the second eigenvalue. This is located, for small angular frequencies, near by the imaginary axis (see Fig. 2) so that again some of the insufficiencies of the RK1 method can be seen. With increasing angular frequency this eigenvalue moves away from the imaginary axis and the precision becomes temporarily better.

4 Modified Discrete-Time Model of an Induction Motor

The problems related to the RK1 method, described in the preceeding section, can of course be avoided by using other efficient integration algorithms. The RK4 algorithm, for example, is well suited for weakly-damped systems [9, 13]. As a special method for the induction motor, a discrete-time model, which switches from the RK1 algorithm for lower frequencies to the Adams-Bashforth algorithm for higher ones, is given in [8]. Series expansions for approximation of the transition matrix are used in [10].

In this paper it should be pointed out that the choice of the continuous-time model to be discretized has already influenced the quality of the discrete-time approximation in a decisive manner, even if the same integration method is used.

The starting point is now eqs. (8) and (9), instead of eqs. (13) and (14). The transformation of stator and rotor flux to a common reference system is skipped at first. Applying the RK1 discretisation to these equations, we obtain

$$\tilde{\psi}_s((k+1)T) = \tilde{\psi}_s(kT) + T\left[-\frac{R_s}{\sigma L_s}\tilde{\psi}_s(kT) + \frac{R_r M}{\sigma L_s L_r}\tilde{\psi}_r(kT) + u_s(kT)\right], \quad (34)$$

$$\tilde{\psi}_r^r((k+1)T) = \tilde{\psi}_r^r(kT) + T\left[-\frac{R_r}{\sigma L_r}\tilde{\psi}_r^r(kT) + \frac{R_r M}{\sigma L_s L_r}\tilde{\psi}_s^r(kT)\right]. \quad (35)$$

The symbol ~ denotes approximations of state variables, matrices and operators related to the method of

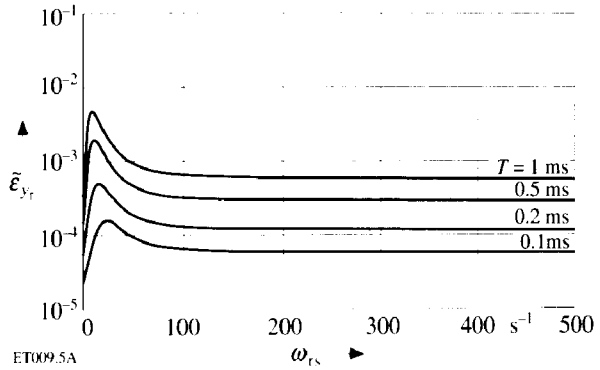

Fig. 5. Error quantity $\tilde{\varepsilon}_{\psi_r}$ of model $(\tilde{\boldsymbol{\Phi}}, \tilde{\boldsymbol{H}})$ versus angular frequency ω_{rs}

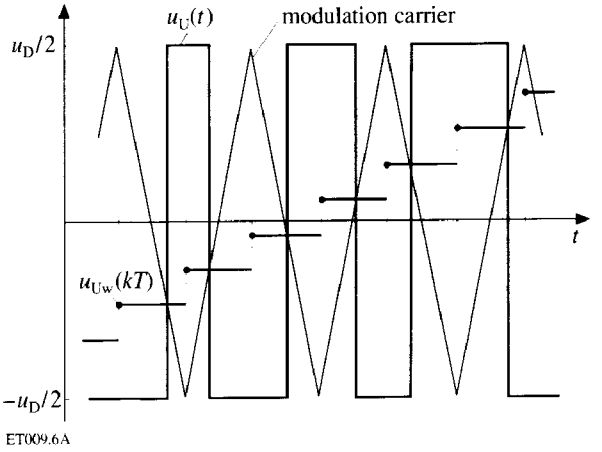

Fig. 6. Pulse-width modulation of phase U with regular sampling method

this section. After discretisation we now transform to a common reference system. For the rotating angle φ_{rs}, which is required for the transformation, we also apply a RK1 discretisation to the deq. (12)

$$\tilde{\varphi}_{rs}((k+1)T) = \tilde{\varphi}_{rs}(kT) + T\omega_{rs}(kT). \tag{36}$$

After carrying out the transformation into the stator reference system, we have

$$\tilde{\psi}_s^s((k+1)T) = \left(1 - T\frac{R_s}{\sigma L_s}\right)\tilde{\psi}_s^s(kT) + T\frac{R_s M}{\sigma L_s L_r}\tilde{\psi}_r^s(kT) + T u_s^s(kT), \tag{37}$$

$$\tilde{\psi}_r^s((k+1)T) = e^{jT\omega_{rs}(kT)}\left[\left(1 - T\frac{R_r}{\sigma L_r}\right)\tilde{\psi}_r^s(kT) + T\frac{R_r M}{\sigma L_s L_r}\tilde{\psi}_s^s(kT)\right]. \tag{38}$$

With that we again obtain a canonical form of eq. (23), whereby now

$$\tilde{\boldsymbol{\Phi}} := \begin{bmatrix} 1 - T\frac{R_s}{\sigma L_s} & T\frac{R_s M}{\sigma L_s L_r} \\ e^{jT\omega_{rs}(kT)} T\frac{R_r M}{\sigma L_s L_r} & e^{jT\omega_{rs}(kT)}\left(1 - T\frac{R_r}{\sigma L_r}\right) \end{bmatrix} \tag{39}$$

appears as approximation of the transition matrix. The approximation of the input matrix

$$\tilde{\boldsymbol{H}} = \hat{\boldsymbol{H}} = \begin{bmatrix} T \\ 0 \end{bmatrix} \tag{40}$$

is identical to the preceeding one.

The error quantity of the rotor flux, corresponding to eq. (33), is evaluated for this model $(\tilde{\boldsymbol{\Phi}}, \tilde{\boldsymbol{H}})$, as well. The results are shown in **Fig. 5**. We recognize approximately the same error as in Fig. 4 in the range of small angular frequencies of model $(\hat{\boldsymbol{\Phi}}, \hat{\boldsymbol{H}})$. For higher frequencies the error is now distinctly smaller. Stability problems do not occur. To get the same dimension of error with the model $(\hat{\boldsymbol{\Phi}}, \hat{\boldsymbol{H}})$ as with the model $(\tilde{\boldsymbol{\Phi}}, \tilde{\boldsymbol{H}})$ also in the higher frequency range, the sampling period must be chosen about 10 times smaller.

5 Simulation

The various models were investigated by means of simulation studies. On the one hand the continuous-time model $(\boldsymbol{A}, \boldsymbol{B})$ and on the other hand both discrete-time models were computed in parallel. For simulating the continuous-time model, the RK4 method was used to get the desired continuous-time behaviour with high precision.

To show a realistic mode of operation, the continuous-time model was fed with a pulsed voltage $u_s^s(t)$ as input signal. This voltage was generated from a reference voltage $u_{sw}^s(t)$ by a pulse-width modulated inverter. In comparison the discrete-time models were fed directly with the reference values $u_{sw}^s(kT)$ as input. Modulation, sampling and timing of reference values are synchronized with each other. The period of the modulation carrier is fixed at twice the sampling time. **Fig. 6** shows this timing (known as "regular sampling" method) for phase U of a three-phase inverter. The complex voltage vector $u_s^s(t)$ is obtained by composition of the three phase potentials [4].

The motor was simulated in steady state with an angular frequency of $\omega_{rs} = 2\pi \cdot 50$ Hz ≈ 314 s^{-1}. The input frequency (frequency of the rotating complex voltage vector) is 319 s^{-1}, that is with positive slip frequency and in motor operation mode. In **Fig. 7**, voltage, current (which is evaluated via eq. (5) from the flux state variables) and rotor flux of the various models are shown as real parts of their complex vectors. The initial values (left margin of diagram) of the discrete-time models are set to those of the continuous-time model. As anticipated, the model $(\hat{\boldsymbol{\Phi}}, \hat{\boldsymbol{H}})$ is unstable. The model quantities (solid lines) quickly depart from the state variables of the continuous-time model.

In comparison, model $(\tilde{\boldsymbol{\Phi}}, \tilde{\boldsymbol{H}})$ accurately approximates the state variables (dotted lines). Because of the chosen sampling period, the discrete-time model cannot detect the current ripple caused by the voltage pulses. Nevertheless, at the sampling instants $t = kT$, the actual current values are met quite well. There is no noticeable ripple in rotor flux due to the low-pass characteristic of the transmission from stator voltage to rotor flux. At the sampling instants the state vari-

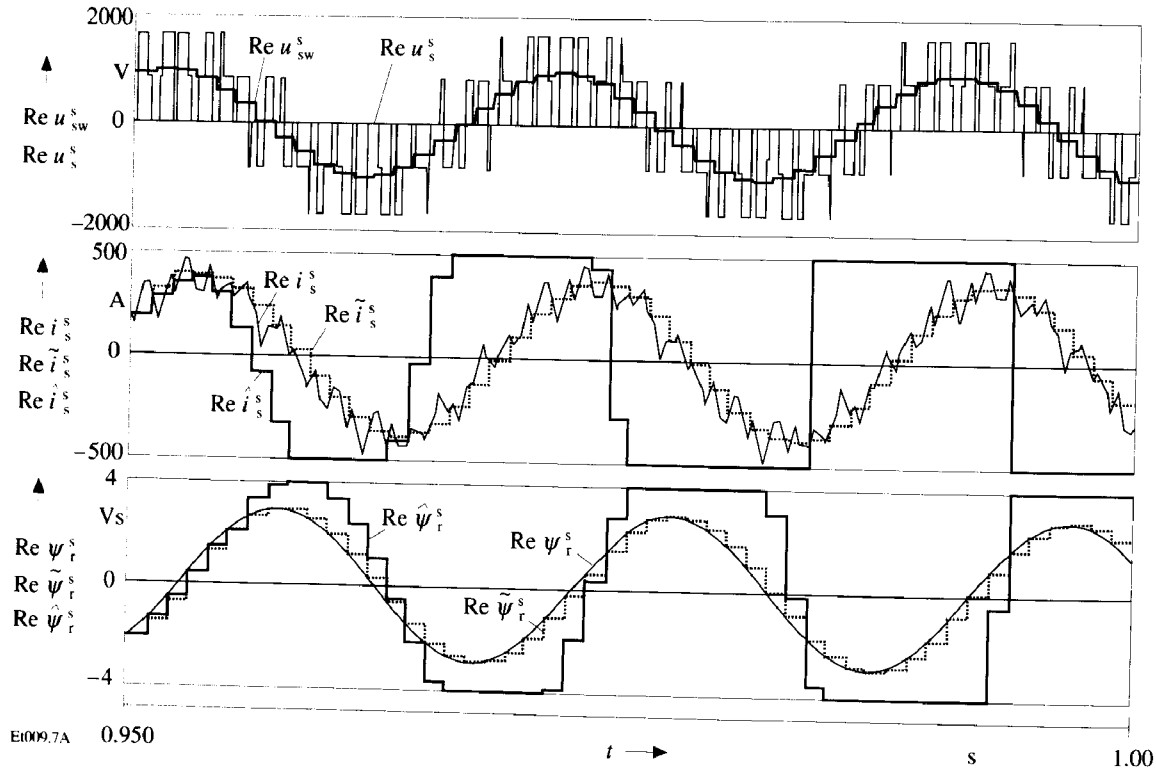

Fig. 7. Simulation results of continuous-time model (A, B) and both discrete-time approximation models ($\hat{\Phi}, \hat{H}$) and ($\tilde{\Phi}, \tilde{H}$)

able $\tilde{\psi}^s_r(kT)$ meets the variable $\psi^s_r(kT)$ of the continuous-time model very well.

6 Discussion

Although both differential eqs. (13) and (14) on the one hand and eqs. (8) and (9) on the other hand are equivalent, the same discretisation method leads to models of totally different quality. The reason is found in the application of the rotation transformation in eq. (10).

Considering the rotor voltage equation only, the transformation of the rotor-referred eq. (9) into stator reference of eq. (14) causes a shifting of the eigenvalue $-1/\tau_r$ of this (decoupled) differential equation by $j\omega_{rs}$. Due to the coupling of the complete system that eigenvalue is obviously displaced only a little (for higher angular frequencies), as can be seen from approximation in eq. (20). From this weakly-damped complex eigenvalue the stability problems involved with the RK1 method in section 3 occur. Hence it seems to be very natural, to skip the transformation first and thus avoid the critical eigenvalue shifting. The discretisation of eq. (9) with real damping is not crucial. The rotation, to which the problem can be traced, is better discretized by approximation of eq. (36).

At this point it should be noticed that the problems of the original discretisation cannot be avoided by choosing the rotor as a common reference system instead of the stator. In this case the voltage eqation of the rotor does not cause any problems at all, but the same problem now occurs with stator voltage equation.

The above results can be applied to other weakly-damped oscillating systems, if weakly-coupled oscillating subsystems can be separated. The eigenvalues of the decoupled subsystems are then displaced only a little by coupling them together as a complete system. Applying a rotation transformation to each of those subsystems with a frequency fixed to the natural frequency (the imaginary part of the concerning eigenvalue), the subsystem can be approximated using a simple discretisation method. After discretisation, the coupling of the subsystems is restored by the inverse rotation transformations.

7 List of Symbols

A	continuous-time system matrix
B	continuous-time input matrix
H	discrete-time input matrix
i	current
I	identity matrix
j	imaginary unit
k	sampling index
L	self-inductance
M	mutual inductance
R	resistance
Re	real part
s_i	eigenvalue of continuous-time system
t	time
T	sampling time
T_{max}	maximum sampling time, which ensures stability
u	voltage

u_w voltage reference value
x state vector
x_i state variable
Γ_i operator of mapping from input u to state variable x_i
ε_i error quantity of approximated state variable x_i
σ leakage coefficient
τ_r rotor leakage time constant
φ_{rs} rotation angle
Φ transition matrix
ψ flux linkage
ω_{rs} angular frequency
$(\tilde{\cdot})$ approximations with RK1 method of section 3
$(\hat{\cdot})$ approximations with modified method of section 4
$(\cdot)_r$ rotor quantities
$(\cdot)_s$ stator quantities
$(\cdot)^r$ rotor reference system
$(\cdot)^s$ stator reference system
$\|\cdot\|_\infty$ L_∞ norm of a sequence or of an operator

References

[1] *Alonge, F.; Raimondi, T.:* Design of a reduced order bilinear observer for induction motors. 7th Int. Conf. Contr. Sys. a. Comp. Sc., Bucharest 1987, Proc. vol. 7, pp. 46–55

[2] *Atkinson, D.J.; Acarnley, P.P.; Finch, J.W.:* Parameter identification techniques for induction motor drives. EPE, Aachen 1989, Proc. pp. 307–312

[3] *Böcker, J.; Hartmann, I.; Zwanzig, C.:* Nichtlineare und adaptive Regelungssysteme. Berlin: Springer, 1986

[4] *Bühler, H.:* Einführung in die Theorie geregelter Drehstromantriebe. Vol. I, Basel: Birkhäuser, 1977

[5] *Franzen, F.; Nelles, D.; Tuttas, C.:* Anschaulische Darstellung einfacher Integrationsalgorithmen. etzArchiv 10 (1988) no. 8, pp. 267–272

[6] *Föllinger, O.:* Lineare Abtastsysteme. München: Oldenbourg, 1974

[7] *Hanselmann, H.:* Diskretisierung kontinuierlicher Regler. Regelungstech. 32 (1984) no. 10, pp. 326–334

[8] *Hodapp, J:* Die direkte Selbstregelung einer Asynchronmaschine mit einem Signalprozessor. Düsseldorf: VDI, Fortschr.-ber. R. 8 (no. 175), 1989

[9] *Jentsch, W.:* Digitale Simulation kontinuierlicher Systeme. München: Oldenbourg, 1969

[10] *Pfaff, G.; Segerer, H.:* Resistance corrected and time discrete calculation of rotor flux in induction motors. EPE, Aachen 1989, Proc. pp. 499–504

[11] *Sattler, P.K.; Stärker, K.:* Control of an inverter fed synchronous machine by estimated pole position. PESC, Kyoto 1988, Proc. vol. III B-2, pp. 415–422

[12] *Stärker, K.:* Sensorloser Betrieb einer umrichtergespeisten Synchronmaschine mittels eines Kalman-Filters. Diss. RWTH Aachen, 1988

[13] *Zurmühl, R.:* Praktische Mathematik für Ingenieure und Physiker. 5. Ed., Berlin: Springer, 1965

Manuscript received on June 18, 1990

The Author

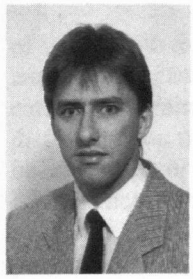

Joachim Böcker (1957) is manager of the control engineering laboratory at the Institute of Drive Systems and Power Electronics of AEG in Berlin/ Ger-many. He studied electrical engineering at the Technical University of Berlin, where he received the Dipl.-Ing. and Dr.-Ing. degrees in 1982 and 1988, respectively. From 1982 to 1987 he was a Research and Teaching Assistant at the 1st Institute of Mechanics, Technical University of Berlin. Main research interests included nonlinear and passive systems. He has been with AEG since 1988. His current interests are associated with digital control of motors and inverters. (AEG AG, Institute of Drive Systems and Power Electronics, Holländerstraße 31 – 34, W-1000 Berlin 51, T +49 30/45 01-3 22)